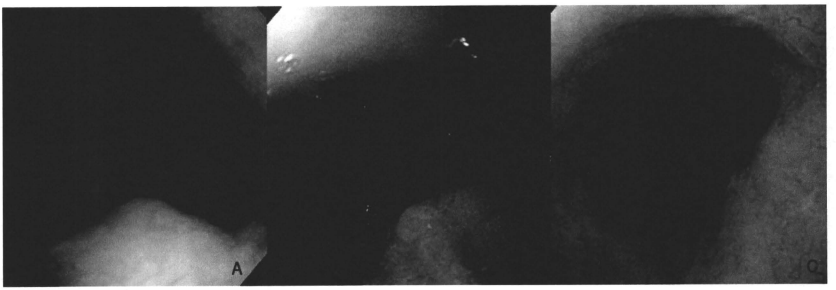

Fig. 1 Initially growing recurrent esophageal cancer at the primary tumor site after complete remission was achieved with chemoradiotherapy may be detected by endoscopy, with features of a submucosal tumor (A), a submucosal tumor with superficial ulcer (B), or a flat erosion (C).

months for 2 years thereafter. Lugol staining and multiple biopsies at the primary site were routinely required.[15] The diagnosis of local recurrence was determined by a positive biopsy.

Of the 133 CR patients, 61 had no recurrence, 56 developed lymph node or distant metastases, and the remaining 16 developed local recurrence at the primary tumor site with no evidence of metastasis. We excluded the 56 patients with lymph node or distant metastases from this study because for them, evaluation of the primary site was not important and only those patients eligible for salvage treatment on local tumors were of interest. Therefore, the endoscopic images of the remaining 77 patients were retrospectively enrolled. This population comprised patients with esophageal squamous cell carcinoma who achieved CR after the initial CRT and developed no metastasis during follow-up, regardless of local recurrence. All of the filed endoscopic images stored after achieving CR, both conventional endoscopy and Lugol-stained chromoendoscopy, were retrospectively collected for reexamination. The stored endoscopic images were evaluated by consensus among three endoscopists experienced in upper gastrointestinal cancer diagnosis (K. T., M. M., K. M.).

RESULTS

Upon the diagnosis of primary-site recurrence for the 16 patients, 13 (81%) had endoscopic findings resembling submucosal tumors (SMT), typically a focal bulge mostly covered by normal-appearing mucosa (Fig. 1A).[16] Eleven of the 13 tumors contained central eroded areas recognized as ulcers or erosions (Fig. 1B and 1C). The remaining three tumors were detected as flat erosions without features of SMT (Table 2).

Images of surveillance endoscopies performed at intervals between CR and the diagnosis of recurrence in the 16 patients were sequentially examined. Newly developed gross lesions at the primary site with negative biopsies were interpreted as recurrent lesions. Evolving lesions were discovered in 13 (81%) patients, including six (38% of the 16 patients) SMT, five (31%) erosions, and two (12%) mild luminal strictures (Table 3).

For all 77 patients achieving CR and free of metastasis, lesions newly developed between CR and the most recent endoscopic surveillance were considered evolving lesions. Therefore, an evolving lesion may be eventually proven to be a recurrence or remain biopsy-negative at the most recent endoscopy. Six of the seven (86%) evolving SMT were subsequently confirmed as recurrent cancer by follow-up

Table 2 Endoscopic findings at primary-site with biopsy-proven recurrence

Endoscopic finding	Number of patients	%
SMT	13	81
SMT with erosion or ulceration	11	
SMT without erosion or ulceration	2	
Erosion	3	19
Total	16	100

SMT, submucosal tumor.

Table 3 Endoscopic findings of newly developed lesion for primary-site recurrent tumors

Preceding newly developed lesions with negative biopsies	Findings at diagnosis of recurrence	Number of patients
SMT	SMT	6
Erosion	SMT	4
Erosion	Erosion	1
Mild stricture	SMT	2
No newly developed lesion	SMT	1
No newly developed lesion	Erosion	2
Total		16

SMT, submucosal tumor.

Table 4 Primary-site biopsy results of the latest surveillance endoscopy for patients who achieved complete remission and remained free of metastasis

Evolving lesion found at preceding endoscopies	Numer of patients (%)	Biopsy result of the latest endoscopy	Number of patients (%)
SMT	7 (9)	Recurrence	6 (86)
		Negative	1 (14)
Erosion	8 (10)	Recurrence	5 (63)
		Negative	3 (37)
Mild stricture	6 (8)	Recurrence	2 (33)
		Negative	4 (67)
No evolving lesion	56 (73)	Recurrence	3 (5)
		Negative	53 (95)
Total	77 (100)		

SMT, submucosal tumor.

endoscopic biopsies. Similarly, five of eight (63%) evolving erosions and two of six (33%) evolving mild strictures were finally confirmed as recurrence. Fifty-six patients were never found to have evolving lesions throughout the follow-up, including three (5%) who were confirmed as recurrence upon the first appearance of an endoscopic lesion. In total, eight of the 21 (38%) patients who developed evolving lesions remained biopsy-negative at their most recent endoscopic follow-up (Table 4).

DISCUSSION

We discovered that the most frequent (81%) endoscopic indicator of primary-site recurrence at its earliest possible stage for a histological diagnosis is SMT. Eighty-one percent of biopsy-proved recurrences were preceded by newly developed lesions such as SMT, erosions, or mild strictures detectable with surveillance endoscopies. Most (86%) evolving SMT with negative biopsies were eventually confirmed as cancer at later endoscopies, but the proportions were lower for other evolving lesions such as erosions (63%) and strictures (33%). This is the first study to describe the morphological changes of early recurring tumors by serial endoscopic observations at short intervals. Our findings will be helpful for improving the skills to detect potentially treatable primary-site recurrence after definitive CRT for esophageal squamous cell carcinoma.

For the endoscopic diagnosis of primary esophageal cancer, several features have been previously described to detect early stage squamous cell carcinoma: localized mucosal erosions in contrast to normal surrounding mucosa; circumscribed mucosal protuberances with irregular configurations; focal areas of mucosal coarsening and congestion; and, rarely, white mucosal plaques.[16] However, these features are not reliable when applied to early recurrent tumors arising from the mucosal bed of a former primary cancer that regressed after CRT. The original esophageal layering and vascular structures have been disrupted by the primary tumor. Furthermore, the expansion and arrangement of recurring neoplastic cells are disrupted by tissue reactions to previous chemotherapy and radiotherapy, as well as by subsequent repair processes. Tumor necrosis, foam cell formation, vascular granulation, inflammatory exudation, and fibrosis are frequent histological sequelae of CRT.[17,18] The minute foci of the initial neoplastic growth may arise from scattered residual cancer cells in deeper tissues, rather than from the superficial mucosal layer, as does the primary cancer.[11] These factors have largely precluded endoscopic ultrasound as a feasible tool in the assessment of residual or recurrent esophageal cancers.[19,20] For the same reason, the endoscopic diagnostic features for recurrent tumors are likely to be different from those for primary tumors.

We speculate that most of the SMT lesions discovered in our study were formed by expanding tumor cells in the submucosal layers, but barely reached the luminal surface because of their depth and constraining fibrosis. Although the overlying mucosa appeared normal, they manifest their first sign by bulging outward. Malignant cells can be captured by biopsy forceps only when they reach the surface in sufficient numbers, or more efficiently, destroy the surface to make an erosion. This might explain why all of the six newly developed SMT yielded negative results at their first biopsies but eventually proved to be recurrences (Table 3).

Several previous studies have aimed to improve the detection of local recurrence by measures other than endoscopy. In addition to pretreatment staging, F-18-fluorodeoxyglucose–positron emission tomography (FDG–PET) is highly sensitive (up to 96%) in detecting recurrent esophageal cancer, but with somewhat lower specificity (68–82%).[21–23] However, its utility in detecting locoregional recurrence is limited by its low specificity (57–75%) for postesophagectomy patients. Postsurgical inflammation and anatomical changes are largely responsible for the false positivity. Detecting small residual or early recurrent cancers is even more challenging because low tumor volume could greatly reduce the sensitivity of FDG–PET. Moreover, such lesions are not distinguishable from post-CRT inflammation or regional lymph-node metastasis.[24,25]

The results of our study disagree with the conventional belief that endoscopy is of limited utility in the management of esophageal cancer after CRT.[13,26] We believe that routine endoscopy, particularly focused on the primary tumor site, is advisable for all patients with esophageal squamous cell carcinoma after the completion of CRT. We also suggest regular endoscopic surveillance at least every three months for those who have achieved CR. The occurrence of

SMT-like lesions after CR is an alarming sign that deserves intensive investigation and follow-up if a modality of salvage treatment is available. Any evolving lesion at the primary site with negative biopsy should be followed closely.

Our retrospective study design has introduced a knowledge bias because the evaluating endoscopists were not totally blinded to the outcomes. Therefore, a randomized controlled trial comparing the clinical outcomes is necessary to establish the role of surveillance endoscopy after definitive CRT for esophageal squamous cell carcinoma.

References

1 Cooper J S, Guo M D, Herskovic A *et al.* Chemoradiotherapy of locally advanced esophageal cancer: long-term follow-up of a prospective randomized trial (RTOG 85-01). JAMA 1999; 81: 1623–7.
2 Suntharalingam M, Moughan J, Coia L R *et al.* The national practice for patients receiving radiation therapy for carcinoma of the esophagus: results of the 1996–1999 Patterns of Care Study. Int J Radiat Oncol Biol Phys 2003; 56: 981–7.
3 Herskovic A, Martz K, al-Sarraf M *et al.* Combined chemotherapy and radiotherapy compared with radiotherapy alone in patients with cancer of the esophagus. N Engl J Med 1992; 326: 1593–8.
4 Kavanagh B, Anscher M, Leopold K *et al.* Patterns of failure following combined modality therapy for esophageal cancer, 1984–90. Int J Radiat Oncol Biol Phys 1992; 24: 633–42.
5 Gill P G, Denham J W, Jamieson G G *et al.* Patterns of treatment failure and prognostic factors associated with the treatment of esophageal carcinoma with chemotherapy and radiotherapy either as sole treatment or followed by surgery. J Clin Oncol 1992; 10: 1037–43.
6 Meunier B, Raoul J, Le Prise E *et al.* Salvage esophagectomy after unsuccessful curative chemoradiotherapy for squamous cell cancer of the esophagus. Dig Surg 1998; 15: 224–6.
7 Swisher S G, Wynn P, Putnam J B *et al.* Salvage esophagectomy for recurrent tumors after definitive chemotherapy and radiotherapy. J Thorac Cardiovasc Surg 2002; 123: 175–83.
8 Nakamura T, Hayashi K, Ota M *et al.* Salvage esophagectomy after definitive chemotherapy and radiotherapy for advanced esophageal cancer. Am J Surg 2004; 188: 261–6.
9 Yano T, Muto M, Minashi K *et al.* Long-term results of salvage endoscopic mucosal resection in patients with local failure after definitive chemoradiotherapy for esophageal squamous cell carcinoma. Endoscopy 2008; 40: 717–21.
10 Yano T, Muto M, Minashi K *et al.* Photodynamic therapy as salvage treatment for local failures after definitive chemoradiotherapy for esophageal cancer. Gastrointest Endosc 2005; 62: 31–6.
11 Mandard A M, Dalibard F, Mandard J C *et al.* Pathologic assessment of tumor regression after preoperative chemoradiotherapy of esophageal carcinoma. Clinicopathologic correlations. Cancer 1994; 73: 2680–6.
12 Brucher B L, Becker K, Lordick F *et al.* The clinical impact of histopathologic response assessment by residual tumor cell quantification in esophageal squamous cell carcinomas. Cancer 2006; 106: 2119–27.
13 Ajani J, Bekaii-Saab T, D'Amico T A *et al.* Esophageal cancer clinical practice guidelines. J Natl Compr Canc Netw 2006; 4: 328–47.
14 Sobin L, Wittekind C. International Union Against Cancer (UICC). TNM Classification of Malignant Tumors, 5th edn. New York: Wiley-Liss, 1997.
15 Mori M, Adachi Y, Matsushima T *et al.* Lugol staining pattern and histology of esophageal lesions. Am J Gastroenterol 1993; 88: 701–5.
16 Silverstein F E, Tytgat G N. Gastrointestinal Endoscopy, 3rd edn. Edinburgh, UK: Mosby, 2002.
17 Darnton S J, Allen S M, Edwards C W *et al.* Histopathological findings in oesophageal carcinoma with and without preoperative chemotherapy. J Clin Pathol 1993; 46: 51–5.
18 Junker K, Thomas M, Schulmann K *et al.* Tumour regression in non-small-cell lung cancer following neoadjuvant therapy. Histological assessment. J Cancer Res Clin Oncol 1997; 123: 469–77.
19 Zuccaro G Jr, Rice T W, Goldblum J *et al.* Endoscopic ultrasound cannot determine suitability for esophagectomy after aggressive chemoradiotherapy for esophageal cancer. Am J Gastroenterol 1999; 94: 906–12.
20 Beseth B D, Bedford R, Isacoff W H *et al.* Endoscopic ultrasound does not accurately assess pathologic stage of esophageal cancer after neoadjuvant chemoradiotherapy. Am Surg 2000; 66: 827–31.
21 Ott K, Weber W, Siewert J R. The importance of PET in the diagnosis and response evaluation of esophageal cancer. Dis Esophagus 2006; 19: 433–42.
22 Flamen P, Lerut A, Van Cutsem E *et al.* The utility of positron emission tomography for the diagnosis and staging of recurrent esophageal cancer. J Thorac Cardiovasc Surg 2000; 120: 1085–92.
23 Kato H, Miyazaki T, Nakajima M *et al.* Value of positron emission tomography in the diagnosis of recurrent esophageal carcinoma. Br J Surg 2004; 91: 1004–9.
24 Nakamura R, Obara T, Katsuragawa S *et al.* Failure in presumption of residual disease by quantification of FDG uptake in esophageal squamous cell carcinoma immediately after radiotherapy. Radiat Med 2002; 4: 181–6.
25 Wieder H A, Brucher B L, Zimermann F *et al.* Time course of tumor metabolic activity during chemoradiotherapy of esophageal squamous cell carcinoma and response to treatment. J Clin Oncol 2004; 22: 900–8.
26 Dittler H J, Fink U, Siewert G R. Response to chemotherapy in esophageal cancer. Endoscopy 1994; 26: 769–71.

Int. J. Radiation Oncology Biol. Phys., Vol. ■, No. ■, pp. 1–5, 2010

0360-3016/$–see front matter

ELSEVIER

doi:10.1016/j.ijrobp.2010.04.071

CLINICAL INVESTIGATION

PROTON BEAM THERAPY AS A NONSURGICAL APPROACH TO MUCOSAL MELANOMA OF THE HEAD AND NECK: A PILOT STUDY

SADAMOTO ZENDA, M.D., MITSUHIKO KAWASHIMA, M.D., TEIJI NISHIO, PH.D., RYOSUKE KOHNO, PH.D., KEIJI NIHEI, M.D., PH.D, MASAKATSU ONOZAWA, M.D, SATOKO ARAHIRA, M.D, AND TAKASHI OGINO, M.D.

Division of Radiation Oncology, National Cancer Center Hospital East, Kashiwa, Chiba, Japan

Purpose: The aim of this pilot study was to assess the clinical benefit of proton beam therapy for mucosal melanoma of the head and neck.

Methods and Materials: Patients with mucosal melanoma of the head and neck with histologically confirmed malignant melanoma and N0 and M0 disease were enrolled. Proton therapy was delivered three times per week with a planned total dose of 60 Gy equivalents (GyE) in 15 fractions.

Results: Fourteen consecutive patients were enrolled from January 2004 through February 2008. Patient characteristics were as follows: median age 73 years old (range, 56 to 79 years); male/female ratio, 7/7; and T stage 1/2/3/4, 3/2/0/9. All patients were able to receive the full dose of proton therapy. The most common acute toxicities were mucositis (grade 3, 21%) and mild dermatitis (grade 3, 0%). As for late toxicity, 2 patients had a unilateral decrease in visual acuity, although blindness did not occur. No treatment-related deaths occurred throughout the study. Initial local control rate was 85.7%, and, with a median follow-up period of 36.7 months, median progression-free survival was 25.1 months, and 3-year overall survival rates were 58.0%. The most frequent site of first failure was cervical lymph nodes (6 patients), followed by local failure in 1 patient and lung metastases in 1 patient. On follow-up, 5 patients died of disease, 4 died due to cachexia caused by distant metastases, and 1 patient by carotid artery perforation cause by lymph nodes metastases.

Conclusions: Proton beam radiotherapy showed promising local control benefits and would benefit from ongoing clinical study. © **2010 Elsevier Inc.**

Proton beam therapy, Mucosal melanoma, Head and neck.

INTRODUCTION

Although rare worldwide, mucosal melanoma of the head and neck is relatively common in Japan (1). Most reports to date have described small series of patients over long time periods but have not led to any consensus in the approach to treatment. A surgical approach incorporating postoperative radiotherapy has been recognized as a community standard, and the 5-year survival rate of head and neck mucosal melanoma varies from 20% to 45% (2–5). This surgical approach is often complicated by serious cosmetic and functional deformity, and, particularly for nasal and sinonasal mucosal melanoma, satisfactory surgical clearance is often markedly difficult to obtain.

Several reports have described the use of radiotherapy alone for mucosal melanoma of the head and neck, with 5-year survival rates slightly less than those of the surgical approach (6–8). Regarding radiotherapy, The review by Trotti *et al.* (9) of four reports of radiotherapy for mucosal melanoma showed 3-year local control rates of 36% to 61%. In Japan Wada *et al.* (10) recently reported a series of 66 cases of mucosal melanoma of the head and neck, 21 of whom were treated with radiotherapy as the main modality. The rate of complete response in these 21 cases was 29%, and the 3-year disease-specific survival rate was 33%. Since X-ray irradiation has a limitation of dose distribution for tumor areas in proximity to organs at risk, like optic nerve and brain stem, it is often difficult to give enough dosage to planned target volume.

Proton beam therapy (PBT) is characterized by rapid fall-off at the distal end of the Bragg peak and a sharp lateral penumbra, depending on the energy, depth, and delivery (11).

Because of its physical characteristics, PBT provides better dose distribution than X-ray irradiation. PBT is deemed a feasible and effective treatment modality that provides curative high-dose irradiation to the tumor volume without increasing normal tissue toxicity. However, the use of PBT

Reprint requests to: Sadamoto Zenda, M.D., Division of Radiation Oncology, National Cancer Center Hospital East, 6-5-1 Kashiwanoha, Kashiwa, Chiba 277-8577, Japan. Tel: (+81) 4-7133-1111; Fax: (+81) 4-7131-9960; E-mail: szenda@east.ncc.go.jp

Conflict of interest: none.

Received Nov 18, 2009, and in revised form March 3, 2010. Accepted for publication April 29, 2010.

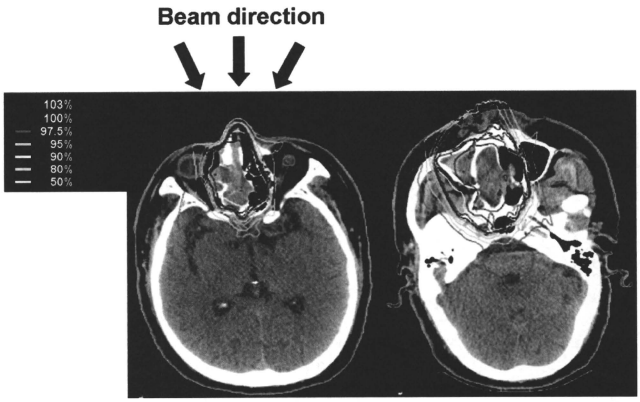

Fig. 1. Target volume and beam arrangement. GTV was defined as the gross tumor lesion determined with pretreatment CT/MRI and PET. CTV was defined as the region of the gross tumor lesion and adjacent sinuses. PTV was basically set as CTV plus 3-mm margin, with acceptance of fine-tuning to the PTV in consideration of organs at risk. Irradiation dose and volume for organs at risk were usually minimized by using a noncoplanar three-field technique.

for mucosal melanoma of the head and neck has not been reported. Here, we conducted a pilot study to examine the utility of hypofractionated PBT as a newly developed treatment modality for mucosal melanoma of the head and neck.

METHODS AND MATERIALS

Patients

Entry criteria for this retrospective study were (*1*) pathologically proven mucosal melanoma of the head and neck; (*2*) clinical TNM status of N0M0; (*3*) Eastern Cooperative Oncology Group (ECOG) performance status of 2 or less; (*4*) adequate organ function; and (*5*) no active concomitant malignancy. This treatment was approved by the institutional review board of the National Cancer Center Hospital, and written informed consent to treatment was obtained from all patients before the initiation of treatment.

Pretreatment clinical evaluation was performed using magnetic resonance imaging (MRI); cervical, chest, and abdominal computed tomography (CT); and/or positron emission tomography-CT (PET-CT). Radiological evaluations for staging were jointly reviewed by radiologists, surgeons, and oncologists at our institution. In the present study, all diseases were staged with the International Union Against Cancer criteria for carcinoma of the nasal cavity or paranasal sinus (12).

Table 1. Patient characteristics

Characteristic	Parameter	No. of patients (n = 14)
Age	Median (range)	73 (56-79)
Gender	Male/female	7/7
Performance Status	0 to 1/2	14/0
Primary site	Nasal cavity	11
	Paranasal sinus	3
TNM stage	T1N0M0	3
	T2N0M0	2
	T3N0M0	0
	T4N0M0	9

Treatment

PBT was delivered three times per week for a planned total dose of 60 Gy equivalents (GyE) in 15 fractions using a 150- to 190-MeV proton beam. The biologically equivalent dose (BED) using a linear-quadratic model is defined as BED = nd [1+ d/1/(α/β)], where n is the fractionation number, d is the daily dose, and the α/β ratio was 2.5 ($Gy_{2.5}$) for malignant melanomas (6). When n = 15 and d = 4 were substituted, BED was 156 $Gy_{2.5}$.

Treatment planning was performed with a three-dimensional CT planning system. In this system, the proton beam was generated with a Cyclotron C235 with an energy of 235 MeV at the exit. Relative biologic effectiveness was defined as 1.1, based on our preclinical

Table 2. Adverse events

	No. of patients with toxicity grade shown*				
Toxicity	1	2	3	4	% 3-4
Dermatitis	7	5	0	0	0
Mucositis	9	2	3	0	21
Infection	0	0	0	0	0
Hearing loss	1	0	0	0	0
Neuropathy					
CN-II	0	0	2	0	12
CN-V	0	0	0	0	0
Keratitis	0	2	0	0	0
Memory impairment	0	0	0	0	0

Treatment-related death: 0%.

* Using Common Terminology Criteria for Adverse Events vesion.3.0.

experiments (13). PBT at our institution is passive irradiation with dual-ring double-scatter methods. Dose distribution was optimized using the spread-out Bragg peak method and obtained using a broad-beam algorithm.

Gross tumor volume (GTV) was determined with pretreatment CT, MRI, and/or PET-CT. The clinical target volume (CTV) was defined as the GTV plus a 5-mm margin and sinuses adjacent to GTV. In cases with brain invasion, the area of T_2-weighted prolongation on MRI was also included in the CTV. The planning target volume (PTV) was basically defined as the CTV plus a 3-mm margin but could be finely adjusted where necessary in consideration of organs at risk. The beam energy and spread-out Bragg peak were fine-tuned such that the PTV encompassed a 90% isodose volume of the prescribed dosage. Irradiation dose and volume for organs at risk was usually minimized using a noncoplanar three-field technique (Fig. 1).

Dose constraints for organs at risk at 4 GyE per fraction were (*1*) surface of brainstem, 45 GyE; (*2*) center of brainstem, 33 GyE; (*3*) optic nerves of the healthy side/chiasm, 42 GyE; and (*4*) optic lens, 13 GyE.

To evaluate the risk of radiation-induced complications in normal tissue, dose–volume histograms were calculated for all patients. Patients were immobilized with custom-made immobilization devices that provided high reproducibility at every treatment fraction. Patient setup was verified before the delivery of each fraction, using a digital radiography subtraction system.

Evaluation of toxicity and efficacy

Toxicities were graded using the Common Terminology Criteria for Adverse Events (CTCAE) version 3.0. Weekly follow-up was continued until acute toxicity was easily manageable, and posttreatment MRI was performed at 6 to 10 weeks after the end of PBT to rule out treatment-induced empyema and brain necrosis. To confirm local control, MRI was performed every 3 to 6 months after the end of treatment, and distant metastases were assessed by CT/PET-CT. The achievement of initial local control was confirmed when all of the following criteria were fulfilled: (*1*) patients were alive at 1 year after the initiation of treatment; (*2*) no progressive disease was detected at the primary site for 1 year; and (*3*) no recurrence was detected at the primary site for 1 year.

Statistical analysis

Overall survival time was calculated from the start of treatment to the date of death or last confirmed date of survival. Survival time was censored at the last confirmed date of survival if the patient was alive. Progression-free survival (PFS) time was defined from the day of initiation of treatment to the first day of confirmation of progressive disease at any site or any cause of death. Overall survival time, PFS time, and local control period were estimated using the Kaplan-Meier product-limits method.

RESULTS

Patient characteristics

Fourteen consecutive patients with mucosal melanoma of the head and neck were treated with PBT at the National Cancer Center East from March 2004 through February 2007. All patients agreed to participate in the present study. Patient characteristics are listed in Table 1. Median age was 72 years (range, 56 to 79 years). Most patients had a good performance status, and over half the patients had T4 disease.

Toxicity

Major adverse reactions to PBT are listed in Table 2. The most common acute toxicities were mucositis (grade 3, 21%) and mild dermatitis (grade 3, 0%). All patients were able to receive the full dose of PBT (60 GyE) given with a median duration of 36 days (range, 33–42 days). Blindness did not occur, although 2 patients had a unilateral decrease in visual acuity. No treatment-related deaths occurred throughout the study.

Efficacy

Initial local control rate was 85.7% (12/14 patients, 95% confidence interval [CI], 57.2%–98.2%). One patient had recurrent disease, and 1 patient died within 1 year after the initiation of treatment.

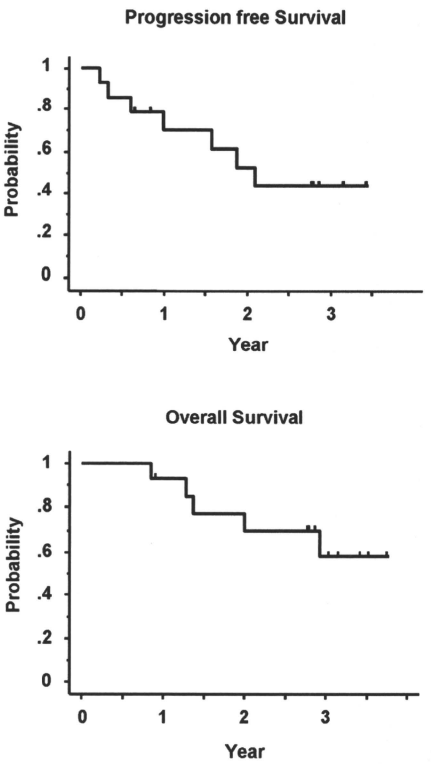

Fig. 2. Progression-free survival (PFS) and overall survival (OS). PFS and OS rates were estimated using the Kaplan-Meier product-limits method. Median PFS was 25.1 months, and 2-year PFS rates were 43.7%. Median survival time was not reached, and 3-year overall survival rate was 58.0% with a follow-up period of 36.7 months.

Table 3. Failure pattern in detail

Case	Time to failure	Failure site	Second-line treatment	Status (time)	Cause of death
1	2.7 M	LN II	Observation	Alive (35.2 M)	
2	22.5 M	LN Ib	Salvage Surgery	Death (35.1 M)	DOD/LM
3	3.8 M	LN Ib, II	Observation	Death (15.4 M)	DOD/DM
6	30.1 M	LN Ib, II	Salvage Surgery	Alive (37.0 M)	
8	11.9M	LN II	Radiation	Death (18.6 M)	DOD/DM
9	7.1 M	LN Ib, II	Salvage Surgery	Death (23.9 M)	DOD/DM
10	8.1 M	Lung	Observation	Death (10.1 M)	DOD/DM
11	18.6 M	Primary site	Observation	Alive (42.7 M)	

Abbreviations: M = months; LN = lymph node; DOD = died of disease; LM = lymph node metastases; DM = distant metastases.

Median PFS was 25.1 months, and 2-year PFS rate was 43.7%. Median survival time with a follow-up period of 36.7 months was not reached, and 3-year overall survival rate was 58.0% (Fig. 2).

Failure pattern and second-line treatment

Six of 14 patients were alive at the end of follow-up with no evidence of disease, while the remaining 8 patients had evidence of disease progression. The most frequent site of first failure was a cervical lymph node outside of the PTV (6/8 patients), followed by local failure in 1 patient (1/8), and lung metastases in one patient (1/8). Failure pattern details are shown in Table 3. With regard to lymph node metastases, 4 patients (4/6) experienced progress within 1 year, and all failure sites were lymph node level Ib or II.

Cause of death

On follow-up, 5 patients died of disease, 4 patients due to cachexia caused by distant metastases and 1 patient by carotid artery perforation cause by lymph nodes metastases.

DISCUSSION

In this study, hypofractionated PBT showed good local control for mucosal melanoma of the head and neck and acceptable toxicity. Prognosis of mucosal melanoma of the head and neck remains poor. In their review of more than 1,000 patients, Mandolis *et al.* (14) reported 5- and 10-year survival rates of 17% and 5%, respectively. Overgaard *et al.* (6) reported a significant relationship between dose per fraction and response, with complete response rates of 59% when fractions of more than 4 Gy were used, compared to 24% with fractions lower than or equal to 4 Gy, while a univariate analysis by Wada *et al.* (9) revealed that a high dose per fraction (3Gy) and high biologically equivalent total dose were associated with better local control and survival.

From these findings, our treatment schedule was planned with consideration for two premises: hypofractionation and high BED. Carbon ion radiotherapy is a promising nonsurgical modality for mucosal melanoma of the head and neck. Yanagi *et al.* (15) reported that with a median follow-up period of 49.2 months, 3-year survival rates were 46.1% in mucosal melanoma patients treated with carbon ion radiotherapy.

The 3-year overall survival rate was 58.0% in the present study. In comparison with the surgical approach or carbon ion therapy, the efficacy of PBT seemed not to be inferior, although recruiting number of patients was small. With regard to late toxicity, decreased visual acuity occurred in 2 patients. Generally, it is often inevitable that the PTV in stage T4 disease with paranasal and/or intracranial invasion includes the unilateral or bilateral optic nerves. In these patients, the better

Table 4. Published cases of late toxicity

Author (study)	Year	Location	Modality	No.of patients	% Treatment outcome	Late toxicity (severe morbidity)
Owens *et al.* (3)	2003	Sinonasal	S	20	5YSR 45%	Not mentioned
			S + RT	24	5YSR 29%	
Temam *et al.* (4)	2005	Sinonasal +α	S/S + RT	30/39	5YSR 20%	Not mentioned
Krengli Owens *et al.* (5)	2006	Head and neck	S/S + RT/others	17/42/15	3YSR 31%	>Grade 3 11% Stenosis of the nasocrimal duct Dry-eye syndrome Optic nerve toxicity Bone necrosis
Wada Owens *et al.* (10)	2004	Sinonasal +α	RT/S+RT	21/10	3YSR 33%	Grade 4 6% soft tissue necrosis; fatal bleeding
Gilligan and Slevin (7)	1991	(Para)-nasal	RT	28	5YSR 17.9%	None
Yanagi *et al.* (15)	2009	Head and neck	Carbon	72	3YSR 46.1%	Grade 2 skin, mucosa*
Present study	2010	Paranasal	Proton	14	3YSR 58.0%	Gade 3 12% unilateral visual acuity

Abbreviations: 5YSR = 5 year survival rate; S = surgery.

* Visual loss after carbon ion radiotheraphy was not mentioned.

dose distribution characteristics of PBT over X-ray should minimize the risk of treatment-related bilateral visual impairment or treatment-related blindness.

Hasegawa *et al.* (16) showed that a certain degree of visual impairment had occurred in 28% of patients whose optic nerves were included in the irradiated volume in carbon ion radiotherapy. There is no report about a direct comparison between PBT and carbon ion radiotherapy.

Previous reports about various approaches to mucosal melanoma are summarized in Table 4.

Cervical lymph nodes were the most frequent site of first failure, and most patients who died finally had distant metastases. Several authors have suggested that aggressive local treatment should be initiated at the presentation of localized melanomas, on the basis that the achievement of local tumor control may increase in survival rate (6, 17). However, it remains controversial whether cervical lymph nodes should be included in the treatment field. We think that what we can do at present is to institute close follow-up after PBT and to detect signs of recurrence or regrowth as early as possible.

CONCLUSIONS

In conclusion, PBT for mucosal melanoma showed promising local control benefit and enough feasibility. To confirm the efficacy and safety, a phase II study of hypofractionated PBT for mucosal melanoma of the head and neck (UMIN-000001505) using the same treatment schedule as the present study is now ongoing in Japan.

REFERENCES

1. Umeda M, Mishima Y, Teranobu O, *et al.* Heterogeneity of primary malignant melanomas in oral mucosa: an analysis of 43 cases in Japan. *Pathology* 1988;20:234–241.
2. Patel SG, Prasad ML, Escrig M, *et al.* Primary mucosal malignant melanoma of the head and neck. *Head Neck* 2002;24:247–257.
3. Owens JM, Roberts DB, Myers JN. The role of postoperative adjuvant radiation therapy in the treatment of mucosal melanomas of the head and neck region. *Arch Otolaryngol Head Neck Surg* 2003;129:864–868.
4. Temam S, Mamelle G, Marandas P, *et al.* Postoperative radiotherapy for primary mucosal melanoma of the head and neck. *Cancer* 2005;103:313–319.
5. Krengli M, Masini L, Kaanders JH, *et al.* Radiotherapy in the treatment of mucosal melanoma of the upper aerodigestive tract: Analysis of 74 cases. A Rare Cancer Network study. *Int J Radiat Oncol Biol Phys* 2006;65:751–759.
6. Overgaard J, Overgaard M, Hansen PV, *et al.* Some factors of importance in the radiation treatment of malignant melanoma. *Radiother Oncol* 1986;5:183–192.
7. Gilligan D, Slevin NJ. Radical radiotherapy for 28 cases of mucosal melanoma in the nasal cavity and sinuses. *Br J Radiol* 1991;64:1147–1150.
8. Sause WT, Cooper JS, Rush S, *et al.* Fraction size in external beam radiation therapy in the treatment of melanoma. *Int J Radiat Oncol Biol Phys* 1991;20:429–432.
9. Trotti A, Peters LJ. Role of radiotherapy in the primary management of mucosal melanoma of the head and neck. *Semin Surg Oncol* 1993;9:246–250.
10. Wada H, Nemoto K, Ogawa Y, *et al.* A multi-institutional retrospective analysis of external radiotherapy for mucosal melanoma of the head and neck in Northern Japan. *Int J Radiat Oncol Biol Phys* 2004;59:495–500.
11. Urie MM, Sisterson JM, Koehler AM, Goitein M, Zoesman J. Proton beam penumbra: Effects of separation between patient and beam modifying devices. *Med Phys* 1986;13:734–741.
12. . Sobin LH, Gospodarowicz MK, Wittekind CH, editors. International Union Against Cancer (UICC): TNM classification of malignant tumors. 7th ed. West Sussex (UK): Wiley-Blackwell; 2010.
13. Ando K, Furusawa Y, Suzuki M, *et al.* Relative biological effectiveness of the 235 MeV proton beams at the National Cancer Center Hospital East. *J Radiat Res (Tokyo)* 2001;42:79–89.
14. Manolidis S, Donald PJ. Malignant mucosal melanoma of the head and neck: Review of the literature and report of 14 patients. *Cancer* 1997;80:1373–1386.
15. Yanagi T, Mizoe JE, Hasegawa A, Takagi R, Bessho H, Onda T, Kamada T, Okamoto Y, Tsujii H. Mucosal malignant melanoma of the head and neck treated by carbon ion radiotherapy. *Int J Radiat Oncol Biol Phys* 2009;1:15–20.
16. Hasegawa A, Mizoe JE, Mizota A, Tsujii H. Outcomes of visual acuity in carbon ion radiotherapy: Analysis of dose-volume histograms and prognostic factors. *Int J Radiat Oncol Biol Phys* 2006;64(2):396–401.
17. Lee SP, Shimizu KT, Tran LM, *et al.* Mucosal melanoma of the head and neck: The impact of local control on survival. *Laryngoscope* 1994;104:121–126.

Int. J. Radiation Oncology Biol. Phys., Vol. ■, No. ■, pp. 1–7, 2010

0360-3016/$–see front matter

ELSEVIER

doi:10.1016/j.ijrobp.2010.05.027

CLINICAL INVESTIGATION

MULTI-INSTITUTIONAL PHASE II STUDY OF PROTON BEAM THERAPY FOR ORGAN-CONFINED PROSTATE CANCER FOCUSING ON THE INCIDENCE OF LATE RECTAL TOXICITIES

KEIJI NIHEI, M.D., PH.D.,* TAKASHI OGINO, M.D., PH.D.,* MASAKATSU ONOZAWA, M.D.,* SHIGEYUKI MURAYAMA, M.D., PH.D.,† HIROSHI FUJI, M.D., PH.D.,† MASAO MURAKAMI, M.D., PH.D.,‡ AND YOSHIO HISHIKAWA, M.D., PH.D.‡

*Radiation Oncology Division, National Cancer Center Hospital East, Kashiwa, Japan; †Proton Therapy Division, Shizuoka Cancer Center, Shizuoka, Japan; ‡Department of Radiology, Hyogo Ion Beam Medical Center, Hyogo, Japan

Purpose: Proton beam therapy (PBT) is theoretically an excellent modality for external beam radiotherapy, providing an ideal dose distribution. However, it is not clear whether PBT for prostate cancer can clinically control toxicities. The purpose of the present study was to estimate prospectively the incidence of late rectal toxicities after PBT for organ-confined prostate cancer.

Methods and Materials: The major eligibility criteria included clinical Stage T1-T2N0M0; initial prostate-specific antigen level of ≤20 ng/mL and Gleason score ≤7; no hormonal therapy or hormonal therapy within 12 months before registration; and written informed consent. The primary endpoint was the incidence of late Grade 2 or greater rectal toxicity at 2 years. Three institutions in Japan participated in the present study after institutional review board approval from each. PBT was delivered to a total dose of 74 GyE in 37 fractions. The patients were prospectively followed up to collect the data on toxicities using the National Cancer Institute-Common Toxicity Criteria, version 2.0.

Results: Between 2004 and 2007, 151 patients were enrolled in the present study. Of the 151 patients, 75, 49, 9, 17, and 1 had Stage T1c, T2a, T2b, T2c, and T3a, respectively. The Gleason score was 4, 5, 6, and 7 in 5, 15, 80 and 51 patients, respectively. The initial prostate-specific antigen level was <10 or 10–20 ng/mL in 102 and 49 patients, respectively, and 42 patients had received hormonal therapy and 109 had not. The median follow-up period was 43.4 months. Acute Grade 2 rectal and bladder toxicity temporarily developed in 0.7% and 12%, respectively. Of the 147 patients who had been followed up for >2 years, the incidence of late Grade 2 or greater rectal and bladder toxicity was 2.0% (95% confidence interval, 0–4.3%) and 4.1% (95% confidence interval, 0.9–7.3%) at 2 years, respectively.

Conclusion: The results of the present prospective study have revealed a valuable piece of evidence that PBT for localized prostate cancer can achieve a low incidence of late Grade 2 or greater rectal toxicities. © 2010 Elsevier Inc.

Proton beam therapy, prostate cancer, radiotherapy, clinical trial, rectal toxicity.

INTRODUCTION

The number of patients with organ-confined prostate cancer has been increasing annually because of the widespread screening using prostate-specific antigen (PSA) measurement and aging society. However, organ-confined prostate cancer can now be cured by radical local treatment, including prostatectomy, external beam radiotherapy (EBRT), or brachytherapy, with or without systemic hormonal therapy.

A total dose of >70 Gy using a standard fractionation schedule is considered to be necessary for EBRT to control the disease (1–3); however, the frequency of normal tissue complications increases when the total dose is >70 Gy for conventional EBRT (4, 5). To deliver higher doses to the prostate without increasing the dose to normal tissues, high-technology EBRT, such as three-dimensional conformal radiotherapy (3D-CRT), intensity-modulated radiotherapy (IMRT), and particle therapy have been developed and

Reprint requests to: Keiji Nihei, M.D., Ph.D., Radiation Oncology Division, National Cancer Center Hospital East, 6-5-1 Kashiwanoha, Kashiwa 277-8577 Japan. Tel: (+81) 4-7133-1111; Fax: (+81) 4-7131-4724; E-mail: knihei@east.ncc.go.jp

Presented in part at the 51st Annual Meeting of the American Society for Therapeutic Radiology and Oncology, September 21–25, 2008, Boston, MA; and at the 48th Meeting of the Particle Therapy Cooperative Group, October 1–3, 2009, Heidelberg, Germany.

Supported in part by the Foundation for the Promotion of Cancer Research in Japan.

Conflict of interest: none.

Received Feb 26, 2010, and in revised form April 30, 2010. Accepted for publication May 14, 2010.

used for more than one decade. Although high-technology techniques of EBRT using X-rays such as 3D-CRT and IMRT have been prospectively evaluated (6–9), the amount of prospective information on the use of proton beam therapy (PBT) alone is limited.

The proton beams used in the modality of particle therapy have distinct physical advantages over conventional photon beams. Proton beams have a low entrance dose, a maximal dose at any prescribed depth called the "Bragg peak," and no exit dose. The "Bragg peak" can be spread out and shaped to conform to the depth and volume of an irregular target. PBT can thus create an inherently three-dimensional conformal dose distribution without exposure of the surrounding normal tissues to excessive doses as compared with the case in conformal photon treatment.

PBT for prostate cancer allows a good dose distribution to be obtained using simple bilateral opposed fields, without exposure of the rectum and bladder to excessive doses. Thus, PBT is theoretically an excellent therapeutic modality owing to its efficacy with reduced toxicity to normal tissues. However, because of the lack of prospective data, it is not yet clear whether PBT can control the incidence of toxicity in the clinical setting. With this background, we started a multi-institutional Phase II trial for patients with organ-confined prostate cancer, focusing on the incidence of late Grade 2 or greater rectal toxicity.

METHODS AND MATERIALS

Patients

The eligibility criteria for inclusion of patients in the present study were (*1*) histologically proven prostate adenocarcinoma, (*2*) clinical Stage II disease (2002 TNM classification, 6th edition, cT1-T2N0M0), (*3*) an initial PSA level of ≤20 ng/mL and Gleason score (GS) of ≤7, (*4*) no history of hormonal therapy or hormonal therapy within 12 months before registration, (*5*) performance status (Eastern Cooperative Oncology Group) 0–2, (*6*) preserved organ function, (*7*) no other active malignancy, and (*8*) written informed consent. Patients with a GS of <7 and PSA level of <10 ng/mL and those with a GS of 7 and/or a PSA level of >10 ng/mL were defined as the low- and intermediate-risk groups, respectively. Patients with Stage cT3-T4, GS 8–10, and/or PSA >20 were not eligible for the present study.

Study endpoints

The primary endpoint was the incidence of late Grade 2 or greater rectal toxicity at 2 years. The secondary endpoints included other toxicities (both acute and late), biochemical relapse-free survival, overall survival, and disease-specific survival. Biochemical failure in the present study was defined as a PSA value of nadir plus 2.0 ng/mL (10, 11), the initiation of any hormonal therapy, or death from any cause.

Study design and statistical analysis

A multi-institutional Phase II study was planned for prospective collection of the toxicity data. The sample size was calculated by the interval estimation method to maintain the accuracy of estimation, using 95% confidence intervals (CIs) of the primary endpoint. The expectation value of the primary endpoint has been defined as <10% according to previous reports of EBRT (12–16). The study sample size was calculated as 150 patients, such that the upper limit of the 95% CI of the primary endpoint was <16% when the actual incidence was <10%. The planned accrual period was 2 years.

Participating institutions

Five institutions were equipped to provide PBT at the beginning of the present study in Japan; three of them participated in the present study, and the institutional review board at each of the three institutions approved the present study (National Cancer Center Hospital East, Kashiwa; Shizuoka Cancer Center, Shizuoka; and Hyogo Ion Beam Medical Center, Hyogo).

Treatment planning

The patients were placed in the supine position and fixed with a vacuum cushion or a thermoplastic cast. The patients were instructed to maintain regular bowel movement; patients with constipation were prescribed laxatives such as magnesium oxide, sennoside, and/or picosulfate sodium to control bowel movement. The bladder filling was controlled by water drinking after urination, and all PBT sessions were performed with a full bladder.

The clinical target volume was defined as the prostate alone for low-risk patients and as the prostate plus the proximal seminal vesicles for intermediate-risk patients, at least encompassing all-known diseases identified by the planning computed tomography scan and other clinical information. The planning target volume consisted of the clinical target volume with optimal margins to account for the uncertainties from the patient setup or internal organ motion, which were estimated at each institution (Table 1). The rectum, from the sigmoid flexure to the anal verge, and the entire bladder as solid organs were delineated as the critical normal structures.

Proton beam therapy

The PBT was delivered at a total dose of 74 GyE in 37 fractions (2 GyE/d). In the low-risk patients, the prostate alone received 74 GyE; in the intermediate-risk patients, a booster dose of 24 GyE was added to the prostate alone after the initial 50 GyE was delivered to the prostate and proximal seminal vesicles. As listed in Table 1, the dose prescription was determined by each institutional method. The dose constraints for the normal tissues were as follows, on the basis of the results from our previous analysis (17) (V_X indicates the percentage of volume receiving more than x GyE): rectum, V_{50} <35%, V_{60} <25%, and V_{70} <15% in the low-risk patients; V_{50} <40%, V_{60} <30%, and V_{70} <20% in the intermediate-risk patients; bladder, V_{65} <50%, V_{70} <35%; femoral head, maximal dose <50 GyE.

Table 1. Details of treatment planning in each institution

Institution	PTV margin (mm)	Dose prescription	Bolus/collimator
NCCHE	7	90% dose to PTV	Individual bolus/ collimator
SCC	5	95% dose to PTV	Individual bolus/ collimator
HIBMC	8–10	To isocenter	No bolus/multileaf collimator

Abbreviations: NCCHE = national cancer center hospital east; SCC = shizuoka cancer center; HIBMC = hyogo ion beam medical center; PTV = planning target volume.

Bilateral opposed fields were used for proton dose delivery. The range modulation by bar-ridge filters was used to generate a spread-out Bragg peak. Proton beams with optimal energy in the range of 190–235 MeV were selected, and individual boluses and collimators were manipulated to conform to the target volume. Daily verification of patient positioning was performed in all patients using orthogonal radiography according to the bony structures. The relative biologic effectiveness of the proton beam was estimated to be 1.1 compared with that of the photon X-rays (GyE = proton Gy × 1.1), in animal experiment conducted at each institution.

Assessments

The registered patients were prospectively followed up to collect data on the toxicities and PSA values at 1 month and once every 3 months after PBT completion for the first 2 years and once every 6 months thereafter.

Late toxicities were defined as those observed >90 days after the start of PBT, but the Radiation Therapy Oncology Group (RTOG)/European Organization for Research and Treatment of Cancer late radiation morbidity scoring scheme was not used in the present study to assess the late toxicities. Instead, so that the observed symptoms could be individually assessed and scored objectively, the National Cancer Institute Common Toxicity Criteria, version 2.0, was used to assess the acute and late toxicities. The symptoms of rectal and/or bladder toxicities assessed in the present study included proctitis, rectal bleeding, rectal pain, hematuria, urinary frequency/urgency, urinary retention, and dysuria (painful urination). Toxicity grading was determined using the severity of each symptom assessed objectively. The Common Terminology Criteria for Adverse Events, version 3.0, was not available when preparing the present study and was not used.

The cumulative incidence of the toxicities and the survival rates were analyzed using the Kaplan-Meier method.

RESULTS

Patients

Between March 2004 and March 2007, 151 patients were enrolled at the 3 institutions for the present study. The patient characteristics are listed in Table 2. Of the 151 patients, 77 and 74 were low- and intermediate-risk, respectively. All the patients enrolled in the present study received the planned PBT up to a dose of 74 GyE in 37 fractions. The median follow-up period was 43.4 months (range, 3–62). Of the 151 patients, 3 were lost to follow-up within the first 2 years, and 1 patient died of other causes on Day 165, without biochemical failure. These 4 patients were excluded from the analysis of late toxicity. All the patients enrolled in the present study were included in the assessment of the acute toxicities and efficacy.

Acute toxicities

The acute rectal and bladder toxicities observed within 90 days of the initiation of PBT are listed in Table 3. All the acute toxicities observed were transient and resolved spontaneously after completion of PBT. No Grade 3 or greater acute toxicities were observed. The rectal toxicities observed included anal pain at defecation, soft stool, anal discomfort, and rectal bleeding. The bladder toxicities were urinary frequency, dysuria, narrow stream, and urinary retention.

Table 2. Patient and tumor characteristics

Characteristic	Value
All patients (*n*)	151
Age (y)	
Median	67
Range	51–82
cT Stage (*n*)	
T1c	75
T2a	49
T2b	9
T2c	17
T3a	1
Gleason score (*n*)	
4	5
5	15
6	80
7	51
iPSA (ng/mL)	
10	102
10–20	49
Hormonal therapy (*n*)	
Yes	42
No	109
Risk group (*n*)	
Low risk	77
Intermediate risk	74

Abbreviation: iPSA = initial prostate-specific antigen.

Late toxicities

The late toxicities at the final follow-up of the 147 patients who had been followed up for >2 years are listed in Table 4. No Grade 3 or greater late rectal toxicities were observed. The late rectal toxicities observed included rectal bleeding, urgency of defecation, and anal pain. The bladder toxicities were transient gross hematuria and urinary retention.

The Kaplan-Meier curves of late rectal and bladder toxicities are shown in Fig. 1. The incidence of late Grade 2 or greater rectal toxicity was 2.0% (95% CI, 0–4.3%) at 2 years (primary endpoint of the present study) and 4.1% (95% CI, 0.4–7.7%) at the final follow-up. The corresponding data for bladder toxicity were 4.1% (95% CI, 0.9–7.3%) at 2 years and 7.8% (95% CI, 2.9–12.8%) at the final follow-up.

Efficacy

The median follow-up period was 43.4 months in the present study. We evaluated the biochemical relapse-free survival

Table. 3. Acute toxicities

Toxicity	Patients (*n*)
Total	151 (100)
Rectum	
Grade 0	135 (89)
Grade 1	15 (10)
Grade 2	1 (0.7)
Bladder	
Grade 0	46 (30)
Grade 1	87 (58)
Grade 2	18 (12)

Data in parentheses are percentages.

Table 4. Late toxicities

Toxicity	Patients (*n*)
Total	147* (100)
Rectum	
Grade 0	115 (78)
Grade 1	27 (18)
Grade 2	5 (3)
Bladder	
Grade 0	128 (87)
Grade 1	9 (6)
Grade 2	8 (5)
Grade 3	2 (1)

Data in parentheses are percentages.
* Number of patients followed up for >2 years.

using the failure definition of nadir plus 2.0 ng/mL; the Kaplan-Meier curve is shown in Fig. 2. Two patients died of other causes on Day 165 and Day 1,202, respectively, without biochemical failure. No patients died of prostate cancer. The biochemical relapse-free survival rate was 94% at 3 years (95% CI, 90–98%).

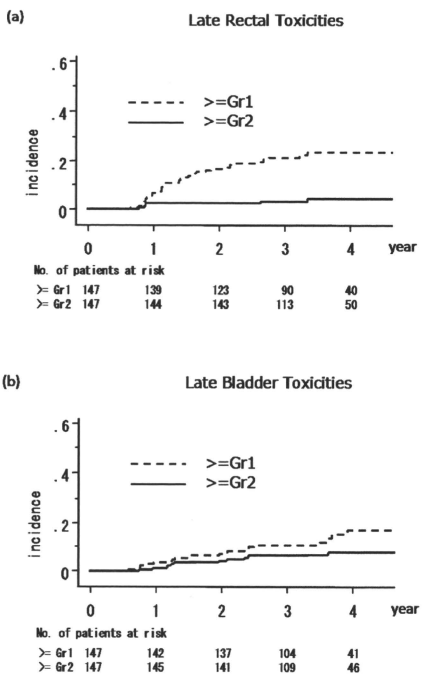

Fig. 1. Kaplan-Meier curves of late (a) rectal and (b) bladder toxicity. Gr = grade.

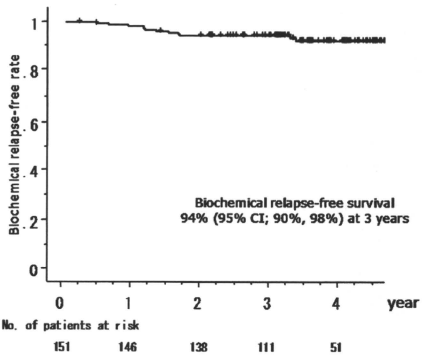

Fig. 2. Biochemical relapse-free survival using definition of nadir plus 2.0 ng/mL. CI = confidence interval.

DISCUSSION

The results of the present prospective study have provided valuable evidence to show a low incidence of late Grade 2 or greater rectal toxicities after PBT for organ-confined prostate cancer. Although PBT is theoretically an excellent modality for EBRT, providing an ideal dose distribution, few well-designed prospective clinical trials are available to corroborate its superiority. The present prospective study was conducted with the aim of scientifically clarifying whether PBT can control the incidence of late rectal toxicity.

The RTOG conducted a Phase I-II dose-escalation study to determine the maximal tolerated dose of 3D-CRT for prostate cancer (RTOG 94-06). The toxicity results of RTOG 94-06 showed a significantly lower incidence of Grade 3 or greater late toxicity but a significantly greater incidence of Grade 2 or less late toxicity than expected from the results of previous RTOG trials (13–15, 18). Although Grade 2 toxicity is generally defined as moderate in severity and is often underestimated, the patients' quality of life can suffer even from such moderate toxicity. Therefore, it is becoming increasingly important to devise sophisticated techniques for high-dose EBRT, such that even the frequency of moderate Grade 2 or less toxicity can be reduced in patients with prostate cancer.

Of the late toxicities that characteristically occur in patients receiving high-dose EBRT for prostate cancer are rectal toxicities, which in most cases, are represented by rectal bleeding, occurring within 2 years of treatment completion. For this reason, the primary endpoint of the present study was defined as the incidence of late Grade 2 or greater rectal toxicity at 2 years after treatment completion.

Since the 1990s, when the existence of a dose–response relationship was suggested in prostate cancer patients undergoing EBRT, dose escalation has been eagerly pursued using high-technology EBRT. In a randomized Phase III trial of 3D-CRT at the M.D. Anderson Cancer Center, the toxicity results revealed an incidence of late Grade 2 or greater

gastrointestinal (GI) toxicity in a high-dose arm (78 Gy in 39 fractions) and standard-dose arm (70 Gy in 35 fractions) of 26% and 12%, respectively (16). Michalski *et al.* conducted a multi-institutional dose-escalation Phase I-II study of 3D-CRT (RTOG 9406; Level 1, 2, and 3, 68.4, 73.8, and 79.2 Gy at 1.8 Gy/fraction; Level 4 and 5, 74 and 78 Gy in 2 Gy/fraction, respectively) and reported the late toxicity profiles at each dose level. Late Grade 2 or greater GI toxicity occurred in 9–13%, 7–9%, 11–14%, 10–16%, and 25–26%, respectively, at dose levels 1–5 (6).

Intensity-modulated RT (IMRT) is a modality of high-technology EBRT. The Memorial Sloan-Kettering Cancer Center has been conducting a single-institutional dose-escalation trial of 3D-CRT and IMRT. Zelefsky *et al.* (7–9) reported that Grade 2 or greater late GI toxicity occurred at an incidence of 16% in patients who had undergone 3D-CRT to a total dose of 75.6–81 Gy (1.8 Gy/fraction). The corresponding incidence was only 2%, even in patients who had undergone IMRT to a total dose of 81–86.4 Gy (7–9). According to a retrospective analysis from the Fox Chase Cancer Center, Grade 2 or greater late GI toxicity occurred at an incidence of 2.4% in patients who had undergone IMRT to a total dose of 74–78 Gy (2 Gy/fraction) (19). However, in some reports, no reduction in the incidence of late toxicity could be achieved despite using IMRT. De Meerleer *et al.* (20) reported that 18% of patients experienced Grade 2 or greater late GI toxicity after receiving a total dose of 74–76 Gy (2 Gy/fractions). Vora *et al.* (21) also reported an incidence of late Grade 2 or greater toxicity of 24% in patients who had undergone IMRT to a total dose of 75.6 Gy.

The PBT facility was installed at Loma Linda University Medical Center in 1990, and the morbidity results for the prostate cancer patients treated to a total dose of 74–75 GyE (1.8–2.0 GyE/fraction) were reported. Late Grade 2 GI toxicity had developed in 21% of the patients at 3 years after treatment completion (22).

The toxicity results in previous reports are summarized in Table 5. The incidence of late Grade 2 or greater rectal toxicity in patients who had undergone 3D-CRT was 9–16% (6, 8). The Memorial Sloan-Kettering Cancer Center and Fox Chase Cancer Center reported a very low incidence of late Grade 2 or greater rectal toxicity (2–2.4%) in patients who had undergone IMRT (7, 9, 19). In contrast, some other centers have reported a high incidence of late rectal toxicity (>15%) even in patients who had undergone IMRT (20, 21). Our results have shown that the incidence of late Grade 2 or greater rectal toxicity was 2.0% at 2 years and 4.1% at the final follow-up; the upper limit of the 95% CIs of these values was 4.3% and 7.7%, respectively. Our results cannot be directly compared with the toxicity data from previous reports, because these studies used different grading scales and also included retrospective and/or single institution-specific data. However, the incidence of late rectal toxicity associated with PBT in the present study was lower than those from the 3D-CRT series and, at least, was not greater than the historical data on the incidence of late Grade 2 or greater GI toxicity after 3D-CRT and IMRT (12–16). The result for the primary endpoint in the present study was 2.0% (95% CI, 0–4.3%) at 2 years, providing at least one piece of scientific evidence of PBT in patients with prostate cancer.

Table 5. Overview of late gastrointestinal toxicity in EBRT for localized prostate cancer

Institution/study	Patients (*n*)	Dose (Gy)	Technique	Grading scale	Grade 1	Grade 2	Grade 3	Follow-up (y)
MDACC (16)	150	70	3D-CRT	RTOG/LENT	36%	11%	1%	6
	151	78			28%	19%	7%	6
					23%, Grade 2/3			2
RTOG 9406 (6)	112	68.4	3D-CRT	RTOG	9-13%, Grade 2/3			9–12
	300	73.8			7-9%, Grade 2/3			7–10
	167	79.2			11-14%, Grade 2/3			9
	256	74			10-16%, Grade 2/3			7–8
	220	78			25-26%, Grade 2/3			6
MSKCC (7–9)	695	75.6–81	3D-CRT	Modified RTOG/CTCAE,	16%, Grade 2/3			5
	561	81–86.4	IMRT	version 3.0	2%, Grade 2/3			7
FCCC (19)	216	74–78	IMRT	Modified RTOG/LENT	2.4%, Grade 2/3			3.5
Ghent University (20)	133	74–76	IMRT	Modified RTOG	47%	17%	1%	3
Mayo Clinic Arizona (21)	145	75.6	IMRT	Modified RTOG	20%	23%	1%	4
LLUMC (22)	643	74	PBT alone	RTOG	—	21%	—	3
		75	X+PBT					
Present study	151	74	PBT alone	NCI-CTC, version 2.0	14%	2.0%, Grade 2/3		2

Abbreviations: EBRT = external beam radiotherapy; MDACC = M.D. Anderson Cancer Center; 3D-CRT, three-dimensional conformal radiotherapy; RTOG = radiation therapy oncology group; LENT = late effects normal tissue task force; MSKCC = memorial sloan-kettering cancer center; IMRT = intensity-modulated radiotherapy; CTCAE = common terminology criteria for adverse events; FCCC = fox chase cancer center; LLUMC = loma linda university medical center; X = photon radiotherapy; PBT = proton beam therapy; NCI-CTC = national cancer institute common toxicity criteria.

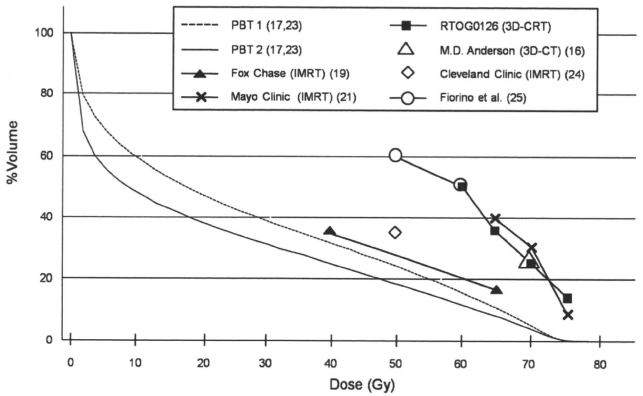

Fig. 3. Average dose–volume histograms (DVHs) for rectum in photon beam therapy (PBT) compared with other dose constraints used in three-dimensional conformal radiotherapy (3D-CRT) or intensity-modulated radiotherapy (IMRT). PBT1 = PBT for intermediate-risk patients; PBT2 = PBT for low-risk patients; RTOG = Radiation Therapy Oncology Group. Data in parentheses indicate reference report.

The previously reported average dose–volume histograms for the rectum in PBT performed at National Cancer Center Hospital East are shown in Fig. 3 (17, 23) and were compared with the other dose constraints used in 3D-CRT or IMRT (16, 19, 21, 24, 25). PBT with simple bilateral opposed fields can thus reduce the dose to the rectum through high to intermediate dose levels, thereby achieving the ideal dose–volume histogram for the rectum. Although bilateral opposed fields can present another issue regarding the dose to the femoral head, the maximal dose to the femoral head in PBT with simple bilateral opposed fields is <35 GyE (45% of the prescribed dose), and V_{30} of the femoral head is <40%.

The total dose of PBT used in the present study was 74 GyE, administered using a conventional fractionation schema (2 GyE/fractions); however, the possible benefit of additional dose escalation and hypofractionation of EBRT for prostate cancer has been suggested, and the efficacy of such a strategy is now under investigation in some randomized trials (16, 26–28). As shown in Fig. 3, the excellent dose–volume histograms for the rectum in PBT might allow the implementation of these strategies; however, additional prospective data are required to ascertain whether PBT administered using these investigational approaches can yield a low frequency of late rectal toxicity.

A more objective grading scale might be necessary to allow comparison of the morbidity data, because different grading scales have been used in previous reports. Thus, the health-related quality of life might be a more rigid and comparable indicator for assessing the toxicities.

Late genitourinary toxicity often occurs after a longer follow-up period (29, 30) and is another issue that needs to be addressed with the use of high-dose EBRT for prostate cancer. As shown in Fig. 1, the incidence curve of late bladder toxicity seems to have been increasing over the years, and that of late rectal toxicity reached a plateau after a few years. Longer follow-up is needed for a more precise assessment of both late genitourinary and GI toxicity.

Quality assurance procedures for clinical assessments have an important role in enhancing confidence in the results of multi-institutional clinical trials. At the beginning of the present study, the specifications for PBT facilities differed among the participating institutions, and the method of delivery of the proton beams to the target organs was defined at the discretion of each institution (Table 1). Although such institutional differences in the method of dose delivery can affect the incidence of toxicity, no significant difference was found in the incidence of toxicity among the three institutions in the present study. Owing to the increasing number of PBT facilities, implementation of quality assurance procedures for PBT in multi-institutional trials, from both the clinical and the physics aspect, is gaining importance.

REFERENCES

1. Perez CA, Walz BJ, Zivnuska FR, *et al.* Irradiation of carcinoma of the prostate localized to the pelvis: Analysis of tumor response and prognosis. *Int J Radiat Oncol Biol Phys* 1980;6:555–563.

2. Hanks GE, Martz KL, Diamond JJ. The effect of dose on local control of prostate cancer. *Int J Radiat Oncol Biol Phys* 1988; 15:1299–1305.

3. Kupelian PA, Elshaikh M, Reddy CA, *et al.* Comparison of the efficacy of local therapies for localized prostate cancer in the prostate-specific antigen era: A large single-institution experience with radical prostatectomy and external-beam radiotherapy. *J Clin Oncol* 2002;20:3376–3385.
4. Pilepich MV, Krall JM, Sause WT, *et al.* Prognostic factors in carcinoma of the prostate—Analysis of RTOG study 75-06. *Int J Radiat Oncol Biol Phys* 1987;13:339–349.
5. Hanks GE. External-beam radiation therapy for clinically localized prostate cancer: Patterns of care studies in the United States. *NCI Monogr* 1988;7:75–84.
6. Michalski JM, Bae K, Roach M, *et al.* Long-term toxicity following 3D conformal radiation therapy for prostate cancer from the RTOG 9406 phase I/II dose escalation study. *Int J Radiat Oncol Biol Phys* 2010;76:14–22.
7. Cahlon O, Hunt M, Zelefsky MJ. Intensity-modulated radiation therapy: Supportive data for prostate cancer. *Semin Radiat Oncol* 2008;18:48–57.
8. Zelefsky MJ, Levin EJ, Hunt M, *et al.* Incidence of late rectal and urinary toxicities after three-dimensional conformal radiotherapy and intensity-modulated radiotherapy for localized prostate cancer. *Int J Radiat Oncol Biol Phys* 2008;70:1124–1129.
9. Zelefsky MJ, Chan H, Hunt M, *et al.* Long-term outcome of high dose intensity modulated radiation therapy for patients with clinically localized prostate cancer. *J Urol* 2006;176: 1415–1419.
10. Roach M III, Hanks G, Thames H Jr., *et al.* Defining biochemical failure following radiotherapy with or without hormonal therapy in men with clinically localized prostate cancer: Recommendations of the RTOG-ASTRO Phoenix consensus conference. *Int J Radiat Oncol Biol Phys* 2006;65:965–974.
11. Thames H, Kuban D, Levy L, *et al.* Comparison of alternative biochemical failure definitions based on clinical outcome in 4839 prostate cancer patients treated by external beam radiotherapy between 1986 and 1995. *Int J Radiat Oncol Biol Phys* 2003;57:929–943.
12. Zelefsky MJ, Fuks Z, Hunt M, *et al.* High-dose intensity modulated radiation therapy for prostate cancer: Early toxicity and biochemical outcome in 772 patients. *Int J Radiat Oncol Biol Phys* 2002;53:1111–1116.
13. Michalski JM, Purdy JA, Winter K, *et al.* Preliminary report of toxicity following 3D radiation therapy for prostate cancer on 3DOG/RTOG 9406. *Int J Radiat Oncol Biol Phys* 2000;46: 391–402.
14. Ryu JK, Winter K, Michalski JM, *et al.* Interim report of toxicity from 3D conformal radiation therapy (3D-CRT) for prostate cancer on 3DOG/RTOG 9406, level III (79.2 Gy). *Int J Radiat Oncol Biol Phys* 2002;54:1036–1046.
15. Michalski JM, Winter K, Purdy JA, *et al.* Preliminary evaluation of low-grade toxicity with conformal radiation therapy for prostate cancer on RTOG 9406 dose level I and II. *Int J Radiat Oncol Biol Phys* 2003;56:192–198.
16. Pollack A, Zagars GK, Starkschall, *et al.* Prostate cancer radiation dose response: Results of the M.D. Anderson phase III randomized trial. *Int J Radiat Oncol Biol Phys* 2002;53:1097–1105.
17. Nihei K, Ogino T, Ishikura S, *et al.* Phase II feasibility study of high-dose radiotherapy for prostate cancer using proton boost therapy: First clinical trial of proton beam therapy for prostate cancer in Japan. *Jpn J Clin Oncol* 2005;35:745–752.
18. Michalski JM, Winter K, Purdy JA, *et al.* Trade-off to low-grade toxicity with conformal radiation therapy for prostate cancer on Radiation Therapy Oncology Group 9406. *Semin Radiat Oncol* 2002;12(Suppl. 1):75–80.
19. Eade TN, Horwitz EM, Ruth K, *et al.* A Comparison of acute and chronic toxicity for men with low-risk prostate cancer treated with intensity-modulated radiation therapy or I 125 permanent implant. *Int J Radiat Oncol Biol Phys* 2008;71:338–345.
20. De Meerleer GO, Fonteyne VH, Vakaet L, *et al.* Intensity-modulated radiation therapy for prostate cancer: Late morbidity and results on biochemical control. *Radiother Oncol* 2007;82:160–166.
21. Vora SA, Wong WW, Schild SE, *et al.* Analysis of biochemical control and prognostic factors in patients treated with either low-dose three dimensional conformal radiation therapy or high-dose intensity-modulated radiotherapy for localized prostate cancer. *Int J Radiat Oncol Biol Phys* 2007;68:1053–1058.
22. Slater JD, Yonemoto LT, Rossi CJ Jr., *et al.* Conformal proton therapy for prostate cancer. *Int J Radiat Oncol Biol Phys* 1998; 42:299–304.
23. Nihei K, Nishio T, Ishikura S, *et al.* Analysis of dose volume histograms in proton therapy for prostate cancer (ECCO [European Cancer Organisation] 12 Abstract Book). *Eur J Cancer Suppl* 2003;1:S161–S162.
24. Kupelian PA, Reddy CA, Klein EA, *et al.* Short-course intensity-modulated radiotherapy (70 Gy at 2.5 Gy per fraction) for localized prostate cancer: Preliminary results on late toxicity and quality of life. *Int J Radiat Oncol Biol Phys* 2001;51:988–993.
25. Fiorino C, Cozzarini C, Vavassori V, *et al.* Relationships between DVHs and late rectal bleeding after radiotherapy for prostate cancer: Analysis of a large group of patients pooled from three institutions. *Radiother Oncol* 2002;64:1–12.
26. Fowler JF, Ritter MA, Chappell RJ, *et al.* What hypofractionated protocols should be tested for prostate cancer? *Int J Radiat Oncol Biol Phys* 2003;56:1093–1104.
27. Kupelian PA, Thakkar VV, Khuntia D, *et al.* Hypofractionated intensity-modulated radiotherapy (70 Gy at 2.5 Gy per fraction) for localized prostate cancer: Long-term outcomes. *Int J Radiat Oncol Biol Phys* 2005;63:1463–1468.
28. Zietman AL, DeSilvio ML, Slater JD, *et al.* Comparison of conventional-dose vs high-dose conformal radiation therapy in clinically localized adenocarcinoma of the prostate: A randomized controlled trial. *JAMA* 2005;294:1233–1240.
29. Gardner BG, Zeitman AL, Shipley WU, *et al.* Late normal tissue sequelae in the second decade after high dose radiation therapy with combined photons and conformal protons for locally advanced prostate cancer. *J Urol* 2002;167:123–126.
30. Lawton CA, Bae K, Pilepich M, *et al.* Long-term treatment sequelae after external beam irradiation with or without hormonal manipulation for adenocarcinoma of the prostate: Analysis of Radiation Therapy Oncology Group studies 85-31, 86-10, and 92-02. *Int J Radiat Oncol Biol Phys* 2008;70:437–441.

Apparent absence of a proton beam dose rate effect and possible differences in RBE between Bragg peak and plateau

Taeko Matsuura[a)]
National Cancer Center Hospital East, 6-5-1 Kashiwanoha, Kashiwa, Chiba 277-8577, Japan

Yusuke Egashira
Department of Bioengineering, Graduate School of Engineering, University of Tokyo, 2-11-16 Yayoi, Bunkyo-ku, Tokyo 113-8656, Japan

Teiji Nishio
National Cancer Center Hospital East, 6-5-1 Kashiwanoha, Kashiwa, Chiba 277-8577, Japan

Yoshitaka Matsumoto, Mami Wada, Sachiko Koike, and Yoshiya Furusawa
Research Center for Charged Particle Therapy, National Institute of Radiological Sciences, 4-9-1 Anagawa, Inage-ku, Chiba-shi, Chiba 263-8555, Japan

Ryosuke Kohno, Shie Nishioka, Satoru Kameoka, Katsuya Tsuchihara, Mitsuhiko Kawashima, and Takashi Ogino
National Cancer Center Hospital East, 6-5-1 Kashiwanoha, Kashiwa, Chiba 277-8577, Japan

(Received 1 June 2010; revised 15 August 2010; accepted for publication 26 August 2010; published 24 September 2010)

Purpose: Respiration-gated irradiation for a moving target requires a longer time to deliver single fraction in proton radiotherapy (PRT). Ultrahigh dose rate (UDR) proton beam, which is 10–100 times higher than that is used in current clinical practice, has been investigated to deliver daily dose in single breath hold duration. The purpose of this study is to investigate the survival curve and relative biological effectiveness (RBE) of such an ultrahigh dose rate proton beam and their linear energy transfer (LET) dependence.

Methods: HSG cells were irradiated by a spatially and temporally uniform proton beam at two different dose rates: 8 Gy/min (CDR, clinical dose rate) and 325 Gy/min (UDR, ultrahigh dose rate) at the Bragg peak and 1.75 (CDR) and 114 Gy/min (UDR) at the plateau. To study LET dependence, the cells were positioned at the Bragg peak, where the absorbed dose-averaged LET was 3.19 keV/μm, and at the plateau, where it was 0.56 keV/μm. After the cell exposure and colony assay, the measured data were fitted by the linear quadratic (LQ) model and the survival curves and RBE at 10% survival were compared.

Results: No significant difference was observed in the survival curves between the two proton dose rates. The ratio of the RBE for CDR/UDR was 0.98 ± 0.04 at the Bragg peak and 0.96 ± 0.06 at the plateau. On the other hand, Bragg peak/plateau RBE ratio was 1.15 ± 0.05 for UDR and 1.18 ± 0.07 for CDR.

Conclusions: Present RBE can be consistently used in treatment planning of PRT using ultrahigh dose rate radiation. Because a significant increase in RBE toward the Bragg peak was observed for both UDR and CDR, further evaluation of RBE enhancement toward the Bragg peak and beyond is required. © *2010 American Association of Physicists in Medicine.* [DOI: 10.1118/1.3490086]

Key words: proton therapy, relative biological effectiveness, dose rate

I. INTRODUCTION

Respiration-gated irradiation system in proton radiotherapy for a moving target, such as lung or liver cancer, requires a long time to deliver fractional dose.[1,2] Also, if the dose escalation is to be realized in the near future, as in the case for carbon therapy,[3,4] the treatment time would have to be prolonged. The prolongation of fractional and overall treatment time possibly increase the risk of treatment error and psychological distress of the patient. Therefore, a short-time high dose rate irradiation protocol is strongly desired.

At the National Cancer Center Hospital East in Japan, an irradiation system for high dose rate therapy (the "one-shot radiation system") has been developed. This system consists of proton image guided radiation therapy system, which enables us to monitor the tumor position during irradiation, and an AVF cyclotron, which has a maximum beam current of 300 nA. A spot scanning system[5] is also under construction, which would allow us to achieve a better DVH for healthy tissues and reduce side effects. For the latter system, high dose rate radiation is achieved by combining the strong intensity beam from the cyclotron and the high-speed scanning technique. If we compare it to the clinical dose rate used to treat liver tumors, which is around 5–8 Gy/min in our institute, the dose rate that we are planning to use in one-shot radiation therapy is more than tenfold higher. The achievable dose rate is even greater in the spot scanning system.

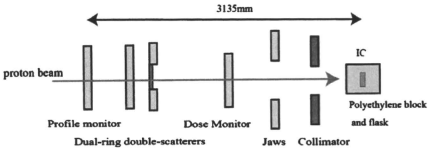

FIG. 1. Schematic figure of the beam line for this experiment.

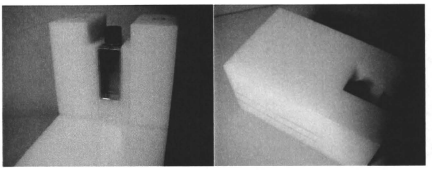

FIG. 2. The flask was placed in a specially molded polyethylene block (0.98 g/cm^3) containing a space to hold it. The thicknesses of the polyethylene block in front of the flask were chosen so that the cells were located at the Bragg peak and plateau, respectively.

In contrast to the technical progress made with our irradiation system, there has been little investigation of the biological response of human cells to high dose rate protons. The relative biological effectiveness (RBE) is one of the most commonly used parameters for characterizing the biological effectiveness of proton beams. Until now, we have been using the same RBE of 1.1 for all doses, dose rates, and linear energy transfers (LETs). This value is in good agreement with that previously measured at spread-out Bragg peak (SOBP) center for SCC61 human squamous cell carcinoma, NB1RGB human fibroblasts, V79 Chinese hamster cells,[6] and human salivary gland (HSG) tumor-originating cells[7] at a dose rate of 1.6–2.7 Gy/min. However, it is not yet clear whether this value could be applied to high dose rate proton therapy. There have been a number of reports on the RBE in ultrahigh dose rate (UDR) regimes using protons provided by tandem accelerator (10^3–10^4 Gy/min for their continuous mode),[8,9] pulse x rays from laser-produced plasma,[10] electron pulse,[11] and the comprehensive literature review about the dose rate effects was done.[12] The former study used protons; however, it was limited to a 3 Gy dose and therefore, no overall survival curve was drawn. The LET dependence of the dose rate effect was also not investigated.

The aim of this study is to clarify whether the biological effectiveness of a high dose rate proton beam is different from that of the present dose rate. Since the LET of protons varies according to the depth of the patient's body being irradiated, data were obtained at multiple LETs. The experiment was performed using HSG cells *in vitro* and the surviving fraction (SF) was determined by a clonogenic assay.

II. MATERIALS AND METHODS

II.A. Beamline and experimental setup

In this experiment, we used the nozzle designed for the dual-ring double scattering method[13,14] in order to obtain flat dose profile and stable dose intensity over the cell containing area. A 235 MeV proton beam produced by an AVF cyclotron was scattered using two thin scatterers on the beamline. These scatterers made it possible to obtain a flat dose profile over the cell containing area ($\pm$2.5% over 2$\times$5 cm^2 field). The beam was then cut off using a 15 cm$\times$15 cm collimator. The experimental setup is shown in Fig. 1.

The HSG cells were placed in the bottom of a slide chamber flask (Lab-Tech SlideFlask 170920, Nunc, Chicago, IL) The flask was then placed in a polyethylene block (0.98 g/cm^3) containing a specially designed space for the flask (Fig. 2). The surface of the cells was placed at the isocenter of the proton beam. In order to obtain the highest dose rate in this setup, as well as to investigate the LET dependence, the flask was placed at the Bragg peak and the plateau of the Bragg curve by placing polyethylene blocks of appropriate thickness in front of the flask. Figure 3 shows the measured/simulated distal dose profile and the LET distribution f(L_D) at the flask positions used in this experiment. The simulation was performed using a GEANT4 toolkit (ver. 4.9.2) and PTSGEOM.[15] Under these conditions, the absorbed dose-averaged LET ($\bar{L}_D$) at the Bragg peak and plateau were 3.19 keV/μm (equivalent to an energy of 15.8 MeV) and 0.56 keV/μm (equivalent to an energy of 146 MeV), respectively.[16]

II.B. Method for calibrating the dose and dose rate

The measurement of the dose and dose rate was conducted with PTW Markus Chambers (Type 23343; PTW, Freiburg, Germany) and an electrometer (FLUKE35040; Fluke Biomedical, Cleveland, OH). Then GafChromic EBT film (International Specialty Products, Wayne, NJ) was used for the verification.

In the following, ultrahigh dose rate (UDR) and clinical dose rate (CDR) represent the dose rates that correspond to a beam current of 45 and 1.5 nA at the entrance of the nozzle, respectively. The corresponding dose rates were 325 and 8 Gy/min at the Bragg peak and 114 and 1.75 Gy/min at the plateau for UDR and CDR, respectively. For CDR, the accuracy of the dose measured by the parallel ion chamber was sufficient. For UDR, however, the ion recombination effect cannot be ignored for both the parallel ion chamber and the dose monitor on the beamline, the latter of which was also an ion chamber. In fact, the ion collection efficiency for UDR was 5% lower than that for CDR. Therefore, we performed the dose measurement for UDR in the following way. First, the lateral dose profile at the depth of the cell position was obtained for the CDR in an extensive region including the point *P*, which was outside of the irradiation field, where the dose was 3% of the dose delivered to the cell containing area. We also measured the dose per monitor unit (DMU) at point *P* for UDR. As the DMU measurement at *P* was reliable even for the UDR, the DMU for the UDR in the irradiation field were obtained from the dose profile for CDR and the DMU at point *P* (see Fig. 4). During the irradiation

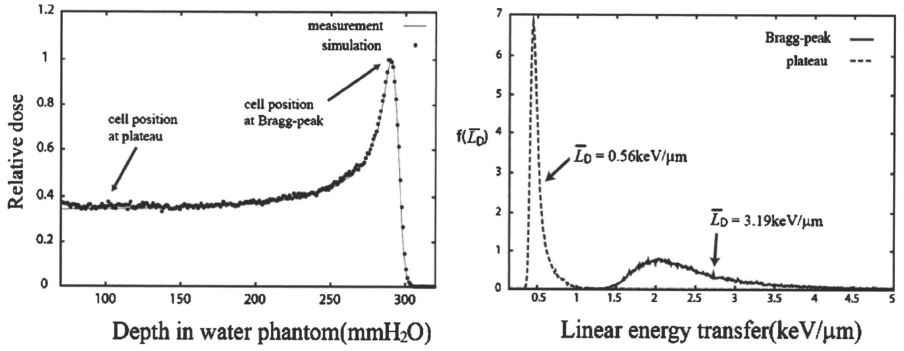

FIG. 3. (Left) Depth-dose profile of the present experiment. The depth-dose measurement was performed in a water phantom. The dots were the results of a GEANT4 simulation. Cell positions are indicated. (Right) The LET distributions at the Bragg peak (solid line) and plateau (dotted line) were calculated by a GEANT4 simulation. In the figure, the distribution has been normalized so that the integral of the distribution $f(L_D)$ is unity.

of the cells, GafChromic EBT film was placed just in front of the each flask and the dose at the moment of irradiation was measured directly. We took advantage of the fact that the optical density (OPD) of the film does not vary with the dose rate, although it does depend on LET.[17] The data points produced by the clinical dose rate were used to determine the OPD dose curve by the weighted least-squares method as follows: $\text{OPD} = A + B \times \exp(-C \cdot \text{dose})$, where A, B, and C are the fitting parameters. The fit was good with a reduced χ-square value of 1.7–2.0. All the data points produced at the ultrahigh dose rate were within one sigma deviation from the OPD curve, which indicates that the abovementioned dose calibration method worked well.

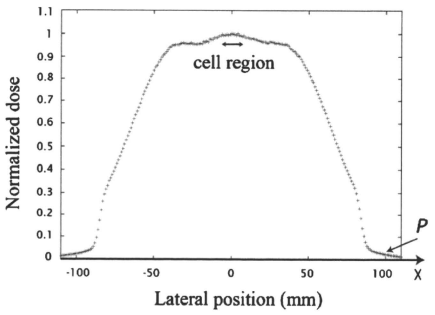

FIG. 4. The lateral dose profile at the cell position depth. The dose was normalized so that the dose at the center of the cell region represented unity. The measurement was performed at the CDR in an extensive region including point $P(x=100)$, which was outside of the irradiation field. The dose at P was 3% of that delivered to the cell containing area. The DMU produced by the UDR at an arbitrary lateral position was determined by the DMU measurement at P for UDR and extrapolation from this profile curve.

In this experiment, in order to obtain a stable proton beam, the timing of the beam initiation was controlled by tuning the radio frequency of the cyclotron. The beam intensity was stabilized to within 4 ms and the variation of the beam current was kept within 2.5% and 15.7% for 45 and 1.5 nA beams, respectively.

II.C. Cell culture and colony formation assay

HSG cells (JCRB1070:HSGc-C5) were used for the experiments. This is a standard reference cell line used for RBE intercomparison of proton facilities in Japan, Korea, etc.[7,18] Eagle's minimum essential medium (M5655, Sigma, Tokyo, Japan) supplemented with 10% fetal bovine serum and antibiotics (100 U/ml penicillin and 100 μg/ml streptomycin) was used as the culture medium.

Subcultured cells were harvested and seeded in a slide chamber flask at about $1.5-2.0 \times 10^5$ cells/flask with 3 ml of the medium and incubated in a 5% CO_2 incubator at 37 °C for 2 days prior to the experiment. The flasks were filled with additional medium 1 day before the experiment and then returned to the incubator.

After being irradiated, the samples were rinsed twice with phosphate buffered saline (PBS), soaked once with 0.025% trypsin, and kept at 37 °C in the remaining trypsin for 4 min before being harvested. The cells were collected in an appropriate volume (2–3 ml) of fresh medium and the cell concentrations were counted by a particle analyzer (Coulter Z1). The cell suspension was diluted using medium, seeded in three 6 cm culture dishes (Falcon 3002) so that there were approximately 100 surviving cells per dish, and incubated in an incubator for 13 days. The colonies in the dishes were rinsed with PBS, fixed with a 10% formalin solution in PBS for 10–15 min, rinsed with tap water, stained with a 1% methylene blue solution, rinsed again with tap water, and

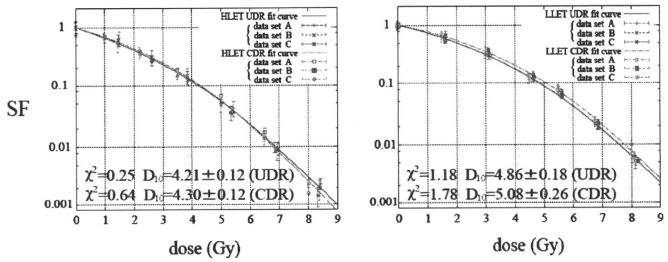

FIG. 5. Survival curves for HSG cells at the Bragg peak (left) and the plateau (right). All data points were fitted by the LQ model. HLET and LLET indicate high and low LET, respectively, and UDR and CDR indicate ultrahigh and clinical dose rate, respectively.

dried in air. Colonies consisting of more than 50 cells were counted under a stereomicroscope as the number of viable cells.

II.D. Analysis of the survival curve and RBE ratios

Doses ranging from 1.0 to 8.0 Gy were delivered at each dose rate and each LET. The irradiation time was 0.2–1.5 s (UDR) and 8–60 s (CDR) at Bragg peak and 0.5–4.2 s (UDR) and 34–274 s (CDR) at plateau, respectively. Three independent cell samples (denoted as A, B, and C) were exposed for each experimental condition. The plating efficiency of unirradiated cells was higher than 80%. In all cases, the surviving fraction is presented as the mean ± standard deviation (SD) of three replicates. The sensitivity coefficients α and β were calculated by curve-fitting all the data using the weighted least-squares method and the LQ-model equation, $SF=\exp(-\alpha D-\beta D^2)$. Here, SF stands for the surviving fraction and D is the absorbed dose to the cells. For the minimization, the Marquardt–Levenberg algorithm was used. D_{10} values (the dose that reduced cell survival to 10%) were obtained from the α and β parameters for each survival data set. From the D_{10} values, we derived the ratios of RBE for different dose rates and LET

$$\mathrm{RRBE(a/b)}=\frac{\mathrm{RBE(a)}}{\mathrm{RBE(b)}}, \tag{1}$$

where a and b indicate UDR and CDR, or high and low LET, respectively. Since we are interested in the variation of RBE over the dose rate, we do not need to use a particular radiation quality as a reference for RBE. The SDs of D_{10} and RRBE value were calculated by the Gaussian error propagation from σ_α and σ_β (SD of α and β, respectively). In addition, differences of estimated SF at D=2, 4, 6, and 8 Gy, which were obtained from the abovementioned curve fitting to the independent data sets (A, B, and C), according to the dose rates and LET were tested with unpaired t-test. The error in absorbed dose was assumed to be negligible.

III. RESULTS

The measured data and fitting curves are illustrated in Fig. 5. The left and right figures show SF at the Bragg peak and plateau, respectively. The reduced χ-square values and the D_{10} values are included in the figure.

At the Bragg peak, the fitted parameters were $\alpha=0.348\pm0.018$ (Gy^{-1}) and $\beta=0.047\pm0.003$ (Gy^{-2}) for UDR and $\alpha=0.294\pm0.019$ (Gy^{-1}) and $\beta=0.056\pm0.003$ (Gy^{-2}) for CDR. The D_{10} value were 4.21 ± 0.12 and 4.30 ± 0.12, respectively, and the ratio of RBE was $\mathrm{RRBE(CDR/UDR)}=0.98\pm0.04$.

At the plateau, the fitted parameters were $\alpha=0.237\pm0.022$ (Gy^{-1}) and $\beta=0.049\pm0.003$ (Gy^{-2}) for UDR and $\alpha=0.183\pm0.029$ (Gy^{-1}) and $\beta=0.053\pm0.005$ (Gy^{-2}) for CDR. The D_{10} value were 4.86 ± 0.18 and 5.08 ± 0.26, respectively, and the RBE ratio was $\mathrm{RRBE(CDR/UDR)}=0.96\pm0.06$, which shows that the dose rate independence of RBE found at the Bragg peak also holds at the plateau.

On the other hand, there are more than 15% differences in RBE between high and low LET for each dose rate: $\mathrm{RRBE(Bragg\ peak/plateau)}=1.15\pm0.05$(UDR) and 1.18 ± 0.07(CDR), indicating that RBE enhancement at the Bragg peak cannot be ignored for both UDR and CDR.

P-values in unpaired t-tests for the difference of SFs according to the dose rates and LET were shown in Table I. There were no statistically significant differences of SFs between CDR and UDR at all above points in Bragg peak and plateau, while significant differences of SFs between Bragg peak and plateau was observed ($p<0.05$).

IV. DISCUSSION

This study revealed that RBE does not depend on the dose rate between 1.75 and 325 Gy/min at the Bragg peak or plateau when it was estimated with SF of HSG cell line. Recently, experiments involving much higher dose rates produced by the Munich tandem accelerator have been performed by Schmid *et al.*[8,9] They irradiated HeLa cells with 3 Gy of laser accelerated 20 MeV protons (equivalent to a dose-averaged LET of 2.66 keV/μm) and obtained RBE of 1.06 ± 0.10 and 1.05 ± 0.11 for two experiments with irradiation times of 100 and 23 ms (the corresponding mean dose rates were estimated to be 1.8 and 7.8 kGy/min), respectively. Although their RBE was not defined in precisely the

TABLE I. Estimated SFs and the P-values in unpaired t-test for the difference of SFs according to the dose rate and LET.

Dose (Gy)	Surviving fraction (standard deviation)				P-values for the difference of surviving fractions			
	Bragg peak		Plateau		UDR vs CDR		Bragg peak vs plateau	
	UDR	CDR	UDR	CDR	Bragg peak	Plateau	UDR	CDR
2	0.423 (0.024)	0.439 (0.016)	0.540 (0.048)	0.550 (0.017)	0.41	0.75	0.02	<0.01
4	0.120 (0.010)	0.122 (0.009)	0.192 (0.025)	0.200 (0.011)	0.76	0.64	0.01	<0.01
6	0.023 (0.003)	0.022 (0.002)	0.045 (0.005)	0.048 (0.005)	0.68	0.47	<0.01	<0.01
8	0.003 (0.001)	0.002 (0.000)	0.007 (0.000)	0.008 (0.001)	0.33	0.38	<0.01	<0.01

same way as ours, our results offered additional data to support that the RBE would not change within the range from the clinical dose rate to ultrahigh dose rate of 7.8 kGy/min. Therefore we submit that the same RBE in CDR is available for one-shot radiation therapy. The reason for the dose rate independence may be that in both our experiment and theirs, the irradiation time scale is much smaller than the repair half time.[19,20] Although we used a mono energy proton beam in this experiment, dose rate independence of the survival curve between high and low LET is also applicable in PRT using SOBP, because LET in the SOBP method distributes the same range as that used in this study.

On the contrary, SFs of HSG cells are substantially dependent on LET. In fact, our data suggested that more than 15% of RBE difference exists between Bragg peak ($\bar{L}_D$=3.19 keV/μm) and plateau ($\bar{L}_D$=0.56 keV/μm). In Bettega *et al.*,[21,22] it was shown that proton RBE determined via the formation of micronuclei in a heteroploid cell line with an epithelioid morphology (EUE line with a modal number of 60 chromosomes) were 1.7, 1.3, and 1.0 for proton beams of 8, 12, and 31 MeV, which had LET of 5.5, 4.0, and 1.8 keV/μm, respectively.[16] Our results, as well as the previous measurement of RBE at SOBP center,[7] were consistent with their results. This study provides additional evidence supporting that there is significant difference of RBE between the Bragg peak and plateau. Since critical organs such as brain stem, cord, and optical nerves are frequently located at the close proximity of the distal fall-off of Bragg peak, the extensive measurement of RBE beyond Bragg peak is urgently required and it should be included in the dose calculation in proton beam treatment planning.[23]

This study may also indicate that we can use the present RBE for scanning proton therapy as long as the dose rate is within the range of that was used in this experiment. In the scanning irradiation, the temporal structure of the dose rate becomes important especially when a rescanning technique is used to attain dose spatial uniformity,[24] but our result showed the temporal variation of the dose rate does not affect the RBE.

A weakness of this study is the fact that in practice, the tissues in the plateau region are different from those in the Bragg peak region, so investigations on one cell line may not tell the whole story. We will investigate this point further in the near future.

V. CONCLUSIONS

We conclude that there were no significant differences in the survival curves of HSG cells produced by proton dose rates of 8 and 325 Gy/min at the Bragg peak ($\bar{L}_D$=3.19 keV/μm) and 1.75 and 114 Gy/min at the plateau ($\bar{L}_D$=0.56 keV/μm) ($p>0.05$). The RBE ratios were RRBE(CDR/UDR)=0.98±0.04 at the Bragg peak and 0.96±0.06 at the plateau. Therefore, the present RBE can be used in therapeutic planning for one-shot radiation therapy. Conversely, significant RBE deviation between high and low LET was found at both the UDR and CDR: RRBE(Bragg peak/plateau)=1.15±0.05(UDR) and 1.18±0.07(CDR). Therefore, RBE enhancement at the Bragg peak and distal fall-off should be carefully considered.

ACKNOWLEDGMENTS

The authors would like to thank Kazutomo Matsumura, Ryuichi Ohta, Hiroyuki Suzuki, Tomohiro Toda, Takeya Taniyama, Takuya Shimoju, Atsushi Sakamoto, and Kenji Yamazaki for their most professional support. T.M. received a grant from the Foundation for the Promotion of Cancer Research.

[a]Author to whom correspondence should be addressed. Electronic addresses: tmk314@gmail.com and matsuura@med.hokudai.ac.jp; Telephone: +81-11-706-5974; Fax: +81-11-706-7876.

[1]K. Nihei, T. Ogino, S. Ishikura, and H. Nishimura, "High-dose proton beam therapy for stage I non-small-cell lung cancer," Int. J. Radiat. Oncol., Biol., Phys. **65**, 107–111 (2006).

[2]M. Kawashima, J. Furuse, T. Nishio, M. Konishi, H. Ishii, T. Kinoshita, M. Nagase, K. Nihei, and T. Ogino, "Phase II study of radiotherapy employing proton beam for hepatocellular carcinoma," J. Clin. Oncol. **23**, 1839–1846 (2005).

[3]H. Tsujii, T. Kamada, M. Baba, H. Tsuji, H. Kato, S. Kato, S. Yamada, S. Yasuda, T. Yanagi, H. Kato, R. Hara, N. Yamamoto, and J. Mizoe, "Clinical advantages of carbon-ion radiotherapy," New J. Phys. **10**, 075009–075024 (2008).

[4]T. Miyamoto, M. Baba, M. Nakajima,. T. Yashiro, K. Kagei, N. Hirasawa, T. Sugawara, N. Yamamoto, M. Koto, H. Ezawa, K. Kadono, H. Tsujii, J. Mizoe, K. Yoshikawa, S. Kandatsu, and T. Fujisawa, "Carbon ion radiotherapy for stage I non-small cell lung cancer using a regimen of four fractions during 1 week," J. Thorac. Oncol. **2**(10), 916–926 (2007).

[5]E. Pedroni *et al.*, "The PSI Gantry 2: A second generation proton scanning gantry," Med. Phys. **14**, 25–34 (2004).

[6]K. Ando, Y. Furusawa, M. Suzuki, K. Nojima, H. Majima, S. Koike, M. Aoki, W. Shimizu, Y. Futami, T. Ogino, S. Murayama, and H. Ikeda, "Relative biological effectiveness of the 235 MeV proton beams at the National Cancer Center Hospital East," J. Radiat. Res. (Tokyo) **42**, 79–89